

Regulation of ubiquitin-dependent cargo sorting by multiple endocytic adaptors at the plasma membrane

Jonathan R. Mayers^a, Lei Wang^a, Jhuma Pramanik^a, Adam Johnson^a, Ali Sarkeshik^b, Yueju Wang^b, Witchuda Saengsawang^c, John R. Yates III^b, and Anjon Audhya^{a,1}

Departments of ^aBiomolecular Chemistry and ^cNeuroscience, University of Wisconsin–Madison School of Medicine and Public Health, Madison, WI 53706; and ^bDepartment of Cell Biology, The Scripps Research Institute, La Jolla, CA 92037

Edited by Pietro De Camilli, Howard Hughes Medical Institute, Yale University, New Haven, CT, and approved June 4, 2013 (received for review February 13, 2013)

Endocytic protein trafficking is directed by sorting signals on cargo molecules that are recognized by cytosolic adaptor proteins. However, the steps necessary to segregate the variety of cargoes during endocytosis remain poorly defined. Using *Caenorhabditis elegans*, we demonstrate that multiple plasma membrane endocytic adaptors function redundantly to regulate clathrin-mediated endocytosis and to recruit components of the endosomal sorting complex required for transport (ESCRT) machinery to the cell surface to direct the sorting of ubiquitin-modified substrates. Moreover, our data suggest that pre-assembly of cargoes with the ESCRT-0 complex at the plasma membrane enhances the efficiency of downstream sorting events in the endolysosomal system. In the absence of a heterooligomeric adaptor complex composed of FCHO, Eps15, and intersectin, ESCRT-0 accumulation at the cell surface is diminished, and the degradation of a ubiquitin-modified cargo slows significantly without affecting the rate of its clathrin-mediated internalization. Consistent with a role for the ESCRT machinery during cargo endocytosis, we further show that the ESCRT-0 complex accumulates at a subset of clathrin-coated pits on the surface of human cells. Our findings suggest a unique mechanism by which ubiquitin-modified cargoes are sequestered into the endolysosomal pathway.

clathrin | multivesicular endosome

The directed movement of proteins and lipids between subcellular organelles is typically mediated by vesicular transport carriers. A variety of coat protein complexes have been shown to promote the membrane deformation steps that are necessary for vesicle biogenesis (1, 2). In particular, the clathrin coat functions at multiple intracellular locations to package a range of cargoes for transport (3, 4). However, clathrin does not engage substrates directly nor does it exhibit the ability to associate with membranes. Instead, recruitment of clathrin is mediated by specific adaptor proteins found on different organelles, which interact with cargoes and lipid bilayers (5). At the plasma membrane, several endocytic adaptors coordinately regulate clathrin accumulation. The best characterized is adaptor protein complex 2 (AP-2), a heterotetrameric adaptor complex that can simultaneously bind to clathrin, sorting signals on cargoes and phosphatidylinositol 4,5-bisphosphate, a lipid specifically enriched on the cell surface (6). Additionally, AP-2 associates directly with other endocytic adaptors including the Eps15 homology (EH) domain containing proteins Eps15 and intersectin, members of the muniscin family such as FCHO1, and the cargo-binding factors Dab2 and Epsin (3, 7, 8). Thus, the AP-2 complex is a multifunctional scaffold that promotes the formation of cargo-laden, clathrin-coated subdomains on the plasma membrane.

Despite its central role in clathrin-mediated endocytosis, the AP-2 complex may not be the first to appear at all future sites of budding. When overexpressed, the FCHO proteins, Eps15, and intersectin may precede the arrival of AP-2 and clathrin on the plasma membrane, although all of these factors exhibit highly similar recruitment kinetics (7, 9, 10). Current models suggest that the FCHO proteins initiate membrane bending and cargo clustering via their FCH-BAR (F-BAR) and μ -homology domains,

respectively (7, 8, 11). Simultaneously, Eps15 and intersectin recruit downstream adaptors and accessory proteins, which collectively drive maturation of the nascent endocytic pit (12). The early recruitment of FCHO1/2, Eps15, and intersectin to the plasma membrane suggest they play a role in the nucleation of clathrin-mediated endocytosis (7, 13). However, this idea remains highly controversial (7, 8, 14).

A large number of cell surface molecules undergo internalization in a clathrin-dependent fashion. This process requires multiple endocytic adaptors to recognize largely distinct cargoes in a manner that relies on short signal sequences or post-translational modifications found within substrates (15). For example, the addition of short ubiquitin chains to transmembrane receptors plays a key role in their sorting from the plasma membrane to the lysosome for degradation (16). The adaptors Eps15 and epsin, which each harbor ubiquitin-binding domains, have been shown to associate with ubiquitin-modified cargoes and direct them into the endolysosomal pathway (17). However, recent studies suggest that the Eps15 ubiquitin interacting motifs may be dispensable for receptor internalization (18). Moreover, yeast cells lacking homologs of Eps15 and epsin continue to remove ubiquitin-modified receptors from the plasma membrane (19). These findings suggest the existence of additional endocytic adaptors that recognize ubiquitin-modified substrates at the cell surface.

Results

A Heterooligomeric Complex of FCHO-1, EHS-1, and ITSN-1 Functions Specifically at the Plasma Membrane in *Caenorhabditis elegans*. To address the function of endocytic adaptor proteins in cargo sorting through the endolysosomal system, we used *C. elegans* as a model system. In contrast to mammalian cells, which express multiple isoforms of the FCHO proteins, Eps15, and intersectin, the *C. elegans* genome encodes single homologs of each adaptor (Fig. S1), which dramatically simplifies functional analysis. To determine the subcellular distributions of these factors during early stages of embryogenesis, we generated a set of affinity-purified antibodies (Fig. 1A), which were used in immunofluorescence studies. Consistent with previous data obtained from cultured cells (7, 8, 14), we found that endogenous FCHO-1, EHS-1, and ITSN-1 localized to the plasma membrane in *C. elegans* embryos (Fig. 1B and Fig. S2A and B). However, there was a notable absence of specific EHS-1 and ITSN-1 staining on intracellular membranes, as was reported for their mammalian counterparts (20). In particular, we failed to observe colocalization of either protein with several, characterized endosomal markers, including EEA-1 and RAB-5 (Fig. 1C). To further verify

Author contributions: J.R.M., L.W., and A.A. designed research; J.R.M., L.W., J.P., A.J., A.S., Y.W., W.S., and A.A. performed research; J.R.Y. and A.A. contributed new reagents/analytic tools; J.R.M., L.W., J.P., A.J., A.S., Y.W., and A.A. analyzed data; and J.R.M. and A.A. wrote the paper.

The authors declare no conflict of interest.

This article is a PNAS Direct Submission.

¹To whom correspondence should be addressed. E-mail: audhya@wisc.edu.

This article contains supporting information online at www.pnas.org/lookup/suppl/doi:10.1073/pnas.1302918110/-DCSupplemental.

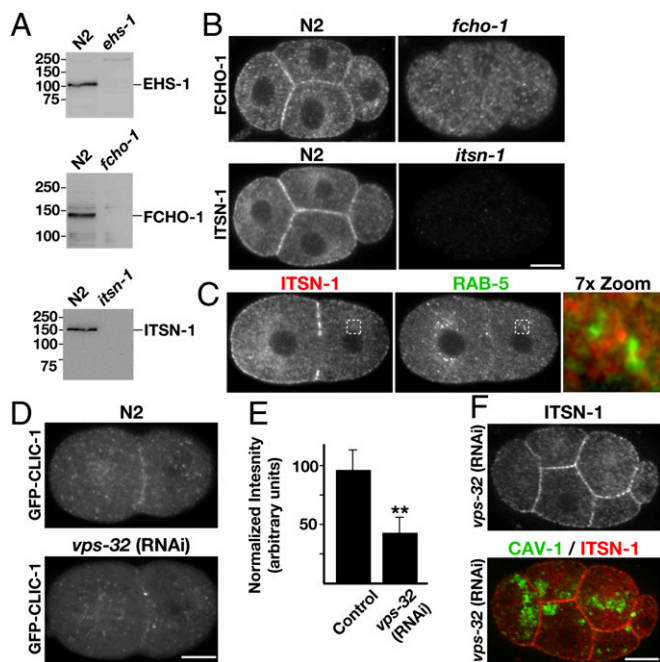


Fig. 1. FCHO-1, EHS-1, and ITSN-1 are plasma membrane-specific adaptor proteins. (A) Whole-worm extracts generated from control (N2) animals and mutant strains were separated by SDS/PAGE and immunoblotted by using affinity-purified antibodies as indicated. (B) Embryos isolated from control hermaphrodites (N2) and strains lacking FCHO-1 (*Top Right*) or ITSN-1 (*Bottom Right*) were fixed and stained by using antibodies directed against each protein. (C) Control embryos were fixed and stained by using antibodies directed against RAB-5 (Cy2; *Left*) and ITSN-1 (Cy3; *Center*). A 7 \times zoom of a boxed region is also provided (*Right*). (D) Control (*Upper*) and VPS-32-depleted embryos (*Lower*) stably expressing a GFP fusion to clathrin light chain (GFP-CLIC-1) were imaged by using swept-field confocal optics. Maximum intensity projections of four cortical sections (2 μ m thick), taken \sim 9 μ m from the coverslip, are shown. (E) Following background subtraction, the total integrated intensity of GFP-CLIC-1 at the cell-cell junction of two-cell stage embryos was calculated (within several 1- μ m² regions) in control and *vps-32*(RNAi) embryos. Representative images are shown ($n = 12$ embryos for each condition). **, significant difference ($P < 0.01$). (F) Embryos expressing GFP-CAV-1 were depleted of VPS-32 by using RNAi and subsequently fixed and stained by using antibodies directed against ITSN-1 and GFP. (Scale bars: 10 μ m.)

the restricted localization of these endocytic adaptors during early embryonic development in worms, we analyzed their distribution in embryos depleted of an ESCRT component (VPS-32), which causes a dramatic alteration in endosome morphology and leads to the aberrant hyperaccumulation of proteins that only transiently associate with endosomal membranes under normal conditions (Fig. S2 C and D; refs. 21 and 22). Although inhibition of ESCRT function resulted in a substantial redistribution of clathrin light chain from the plasma membrane (Fig. 1 D and E), localization of the endocytic adaptors was unaffected (Fig. 1 F and Fig. S2 E). Based on these collective findings, we conclude that FCHO-1, EHS-1, and ITSN-1 are enriched on the plasma membrane but largely absent from endosomes.

The FCHO proteins have been suggested to act as major interaction hubs, which bind to multiple factors that contribute to clathrin-mediated endocytosis, including Eps15 and intersectin (7–9, 11, 13). To determine whether native FCHO-1 associates stably with EHS-1 and ITSN-1, we separated a *C. elegans* embryo extract by using size exclusion chromatography and determined the elution profiles of each endocytic adaptor. We found that FCHO-1 cofractionated with both EHS-1 and ITSN-1 in two unique peaks, suggesting that the three proteins coassemble into at least two distinct complexes in vivo (Fig. 2 A and B). Interestingly, the larger

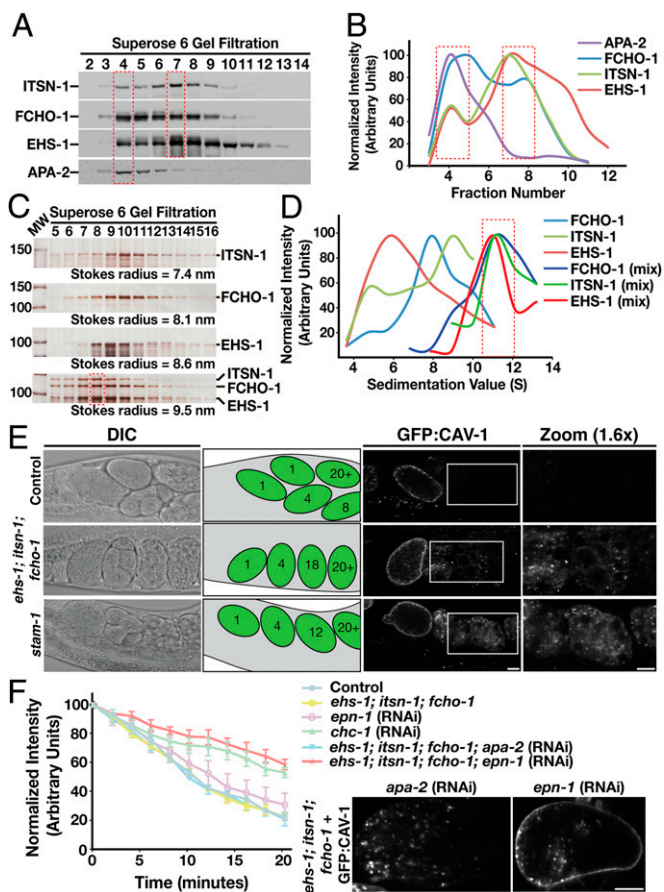


Fig. 2. FCHO-1, EHS-1, and ITSN-1 form a stable complex that functions in the trafficking of ubiquitin-modified cargoes to the lysosome for degradation. (A) An embryo extract was separated by gel filtration chromatography, and eluted fractions were immunoblotted by using antibodies directed against ITSN-1, FCHO-1, EHS-1, and APA-2. Based on densitometry measurements, peak fractions were identified for each protein (boxed regions). (B) Graphical representation of densitometry measurements conducted on immunoblots shown in A. (C) Recombinant ITSN-1, EHS-1, and FCHO-1 were applied individually or as a mixture onto a gel filtration column, and eluted fractions were separated by SDS/PAGE before silver staining. The Stokes radius for each protein was calculated based on the elution profiles of characterized standards. (D) Recombinant ITSN-1, EHS-1, and FCHO-1 were applied individually or as a mixture onto glycerol gradients (10–30%), which were centrifuged and fractionated. Each fraction was separated by SDS/PAGE and silver stained. Densitometry measurements, which are shown in a graphical representation, were used to define the sedimentation value of each protein (boxed region). (E) Immobilized control, *ehs-1;itsn-1;fcho-1* triple mutant animals, and *stam-1* single mutant animals expressing GFP-CAV-1 were imaged by using DIC (*Left*) and swept-field confocal optics (*Right*). Cartoons highlighting the number of cells contained within each embryo observed in utero are provided (*Center*). Additionally, a 1.6 \times zoom of a boxed region within the uterus of each animal is also shown. (F) The rates of GFP-CAV-1 endocytosis from the plasma membrane following ovulation were analyzed in control (N2) or *ehs-1;itsn-1;fcho-1* triple mutant embryos by measuring the loss of cell surface fluorescence over time in utero ($n = 5$ for each condition). In some cases, animals were depleted of epsin (*epn-1*), APA-2, or clathrin heavy chain (*chc-1*) as indicated. A comparison of GFP-CAV-1 localization in one cell stage *ehs-1;itsn-1;fcho-1* triple mutant embryos (during metaphase) following APA-2 or EPN-1 depletion is also shown (*Right*). (Scale bars: 10 μ m.)

peak also contained subunits of the AP-2 complex, which has been shown to associate with Eps15, intersectin, and FCHO1 (7, 8). Thus, our data indicate that FCHO-1, EHS-1, and ITSN-1 form a complex that is capable of existing independently or in association with the AP-2 complex.

To confirm that FCHO-1, EHS-1, and ITSN-1 assemble into a stable complex, we expressed each full-length protein recombinantly and assayed their ability to bind to one another. Individually, each adaptor protein exhibited a distinct elution profile following gel filtration chromatography (Fig. 2C). However, when mixed together, the three proteins coeluted as a single complex with an average Stokes radius of 9.5 nm (Fig. 2C). They also remained associated during sedimentation velocity centrifugation, exhibiting an S value of 10.8 S (Fig. 2D). Based on its hydrodynamic properties (23), we estimated the native molecular mass of the complex to be ~430 kDa. Together, these data indicate that FCHO-1, EHS-1, and ITSN-1 form a stable heterooligomeric complex on the plasma membrane, which we refer to as the FEI adaptor complex.

The FEI Adaptor Complex Regulates Protein Sorting in the Endolysosomal Pathway. Endocytic adaptors play a key role in cargo selection (5, 6, 15, 16, 24). To investigate a potential role for components of the FEI complex in ubiquitin-dependent protein sorting in *C. elegans*, we used previously isolated strains containing deletion mutations in each gene (Fig. S1B). In contrast to the essential roles of the FCHO proteins, Eps15, and intersectin in other species (7, 8, 25), null mutations in each gene failed to substantially impact *C. elegans* viability or embryonic development (Table S1).

We next analyzed the effect of each loss-of-function mutation on the trafficking of CAV-1, the *C. elegans* homolog of caveolin-1, which was shown to undergo clathrin-mediated endocytosis and ubiquitin-dependent transport to the lysosome for degradation (26, 27). In the proximal oocytes of control animals, CAV-1 resides on Golgi-derived cortical granules, which fuse en masse with the plasma membrane following fertilization and ovulation. CAV-1 is subsequently internalized and ubiquitin-modified during the one-cell stage of embryonic development and rapidly degraded in an ESCRT-dependent manner (Fig. 2E and Fig. S2F; refs. 21 and 26). Individual loss of function mutations in FCHO-1, EHS-1, or ITSN-1 failed to elicit a defect in CAV-1 trafficking and degradation (Fig. S2G). To determine whether components of the FEI complex may function redundantly in cargo sorting, we generated mutant strains lacking multiple components. We found that animals lacking all three subunits exhibited a significant delay in CAV-1 degradation and enhanced embryonic lethality compared with the single and double mutant strains (Fig. 2E, Fig. S2G, and Table S1). Importantly, this effect was not a result of disrupted clathrin or AP-2 recruitment to the plasma membrane (Fig. S2H and I). Instead, these data suggest that FCHO-1, EHS-1, and ITSN-1 directly regulate the sorting of ubiquitin-modified cargoes and can partially substitute for one another during early *C. elegans* development. Additionally, our findings argue against a model in which FCHO proteins act as nucleating factors for clathrin-mediated endocytosis.

A delay in CAV-1 degradation could arise from either impaired endocytosis at the plasma membrane or a subsequent defect in cargo sorting to the lysosome. To discriminate between these possibilities, we analyzed the rate of GFP-CAV-1 internalization based on changes in its fluorescence intensity at the plasma membrane following ovulation. Surprisingly, we found that embryos lacking all three FEI subunits did not exhibit a significant defect in CAV-1 endocytosis compared with control eggs (Fig. 2F and Movies S1 and S2). Instead, CAV-1 remained associated with Rab5-positive early endosomes for an extended period in mutant embryos, which was not observed in control animals (Fig. S3A), but was reminiscent of the defect observed in animals lacking the function of one or more components of the ESCRT machinery (Fig. 2E; ref. 21).

To determine whether alternative endocytic factors function in CAV-1 endocytosis, we individually depleted all known *C. elegans* clathrin adaptors, including homologs of human stonin (UNC-41), AP180/CALM (UNC-11), the alpha subunit of AP-2 (APA-2), Disabled (DAB-2), NUMB (NUM-1), and epsin (EPN-1) and examined trafficking of CAV-1 (Fig. S3B). Although we failed to identify changes in the rate of CAV-1 internalization following

individual depletion of these components in otherwise wild-type animals, we found that inhibition of EPN-1 in animals lacking all components of the FEI complex specifically caused a potent inhibition of CAV-1 endocytosis, similar to that observed following depletion of clathrin heavy chain (Fig. 2F and Fig. S3B). Collectively, these data indicate that subunits of the FEI complex act redundantly to regulate multiple steps of cargo sorting at the plasma membrane and potentially recruit additional adaptors that function in the endolysosomal trafficking of ubiquitin-modified membrane proteins.

In addition to our analysis of CAV-1, we further defined the role of the FEI complex in the trafficking of MIG-14, a characterized clathrin-dependent cargo that recycles instead of being degraded in the lysosome and, thus, is unlikely to be ubiquitin-modified (28). During fertilization and ovulation, MIG-14 is largely internalized in control embryos (Fig. S3C and D and Movie S3). However, in embryos lacking all components of the FEI complex, significantly higher levels of MIG-14 are observed on the plasma membrane (Fig. S3C and D and Movie S4), although its endocytosis is not entirely blocked. These data further support our findings demonstrating that the FEI complex acts redundantly with other adaptors during cargo internalization, likely together with AP-2 in this case, which was implicated in MIG-14 endocytosis (29). Importantly, movement of MIG-14 through endosomal compartments was not delayed in the triple *fcho-1;ehs-1;itsn-1* mutant strain, consistent with the idea that the function of the FEI complex is limited to the cell surface (Fig. S3D and E).

The FEI Complex Interacts Directly with ESCRT-0 at the Plasma Membrane.

To identify additional cargo adaptors that function together with the FEI complex, we took advantage of antibodies directed against EHS-1 and ITSN-1 to conduct a series of immunoprecipitations from *C. elegans* embryo extracts. Using solution mass spectrometry and immunoblot analysis, we reproducibly isolated a set of factors known to function during endocytic protein transport, including all components of the FEI complex, clathrin heavy and light chains, members of the AP-2 adaptor complex, and both subunits of the ESCRT-0 complex (STAM-1 and HGRS-1; Fig. S4A and Table S2). Reciprocal immunoprecipitations using STAM-1 and HGRS-1 antibodies confirmed the existence of this interaction network (Fig. S4A and Table S2). Additionally, we found that a subpopulation of native STAM-1 and HGRS-1 cofractionate with the AP-2 and FEI complexes following size exclusion chromatography of a *C. elegans* embryo extract (Fig. S4B). Notably, we failed to observe associations between components of the FEI complex and other ESCRT subunits, suggesting that the interaction with ESCRT-0 was specific (Table S2). These data indicate that the FEI complex, potentially in concert with AP-2 and clathrin, binds to ESCRT-0.

Previous studies suggest that mammalian ESCRT-0 binds specifically to a short isoform of Eps15 (Eps15b) that lacks amino-terminal EH domains, localizes only to endosomes, and does not interact strongly with the AP-2 complex (30). In contrast, our data indicate that *C. elegans* ESCRT-0 interacts with a plasma membrane isoform of EHS-1 that also coimmunoprecipitates with components of the AP-2 complex. To further validate the interaction, we generated GST fusions to three partially overlapping regions of EHS-1 and tested their ability to associate with native ESCRT-0. Our findings demonstrated that the amino-terminal EH domains of EHS-1 bound specifically to ESCRT-0 (Fig. S4C). We confirmed this association using the GST fusions and recombinant STAM-1, indicating that EHS-1 binds directly to the ESCRT-0 complex (Fig. S4D). To determine whether ITSN-1 and FCHO-1 also associate with ESCRT-0, we generated recombinant fragments of each protein for interaction studies. We found that both the coiled-coil and SH3 domains of ITSN-1 bound to ESCRT-0 directly (Fig. S4E and F). Additionally, we found that the middle and μ -homology domains of FCHO-1 bound to ESCRT-0 under similar conditions (Fig. S4F). Together, these studies indicate that multiple components of the FEI complex associate with ESCRT-0.

Our data indicate that the FEI complex localizes to the plasma membrane, suggesting that an association with ESCRT-0 would be restricted to that site. To investigate this possibility, we conducted immunofluorescence studies using HGRS-1 and STAM-1 antibodies. Consistent with previous findings (31), imaging of the one-cell stage embryo (away from the cell surface) revealed that both components of ESCRT-0 localize to endosomes (Fig. 3A). However, we additionally observed an accumulation of each protein at or near the plasma membrane, which was most obvious in multicellular embryos (Fig. 3B). In contrast, we failed to observe a similar cell surface localization of other endosomal proteins, including EEA-1 (Fig. 3C). To determine whether the cell surface distribution of ESCRT-0 depends on the presence of the plasma membrane-associated endocytic adaptor proteins, we examined its localization in a variety of mutant backgrounds. Strikingly, in triple mutant animals lacking all components of the FEI complex, ESCRT-0 localization to the plasma membrane was dramatically reduced, although not completely abolished (Fig. 3D and Fig. S5A). Because the ESCRT-0 plasma membrane interaction network also included the AP-2 complex, we examined the effect of depleting APA-2 by using RNA interference (RNAi) in control animals. Under these conditions, we observed a relatively minor diminution in ESCRT-0 localization at the cell surface (Fig. 3D). To determine whether the AP-2 and FEI complexes function redundantly in targeting ESCRT-0, we depleted APA-2 in animals lacking FCHO-1, EHS-1, and ITSN-1. In the absence of these four components, we observed a dramatic defect in ESCRT-0 recruitment to the plasma membrane (Fig. 3D). Additionally, embryonic viability was reduced significantly under these conditions, highlighting the overlapping roles of the FEI and AP-2 complexes during *C. elegans* embryogenesis (Table S1). Taken together, these data strongly suggest that multiple endocytic adaptor complexes function to recruit ESCRT-0 to the cell surface to engage ubiquitin-modified substrates at the plasma membrane.

A major determinant for ESCRT-0 localization is its affinity for phosphatidylinositol 3-phosphate (PI3P), which is enriched on early endosomes (32). However, additional anionic phospholipids also participate in targeting FYVE domain-containing proteins (33). To determine whether the ESCRT-0 complex can also bind to membranes that are devoid of PI3P, we conducted a series of liposome coflotation assays. We found that the presence of 15% phosphatidylserine (PS) in liposomes, similar to the concentration of negatively charged phospholipids in the plasma membrane (34), is sufficient to promote membrane association of ESCRT-0 (Fig. 4A). These data suggest that a combination of lipid- and protein-dependent associations can promote ESCRT-0 localization to the cell surface.

ESCRT-0 Associates with Clathrin-Coated Pits in Human Cells. Based on its interactions with endocytic adaptor proteins at the plasma membrane, we investigated the possibility that ESCRT-0 is recruited specifically to sites of clathrin-mediated endocytosis. To do so, we used total internal reflection fluorescence (TIRF) microscopy to visualize both clathrin and ESCRT-0 at the cell surface of mammalian tissue culture cells. Following transient transfection of a construct encoding RFP-clathrin light chain (RFP-LCa) into HeLa cells stably expressing a low level of YFP-Hrs, we identified numerous sites of clathrin-coated pit formation on the plasma membrane (Fig. 4B). Consistent with previous work (10), some of these sites exhibited a short lifetime (in the 60- to 90-s range), whereas others persisted for several minutes. Two-color TIRF imaging revealed that YFP-Hrs colocalized with a subpopulation (~27%) of clathrin-coated structures (Fig. 4B; $n = 641$ sites analyzed). Importantly, overexpression of YFP-Hrs that was sufficient to alter endosome morphology (Fig. S5B) did not significantly increase the percentage of clathrin-coated pits that exhibited the presence of ESCRT-0. Time-lapse analysis further demonstrated that Hrs accumulation at the plasma membrane did not precede or coincide with the initial arrival of clathrin light chain (Fig. 4C and D). However, disappearance of Hrs occurred simultaneously with the movement of clathrin out

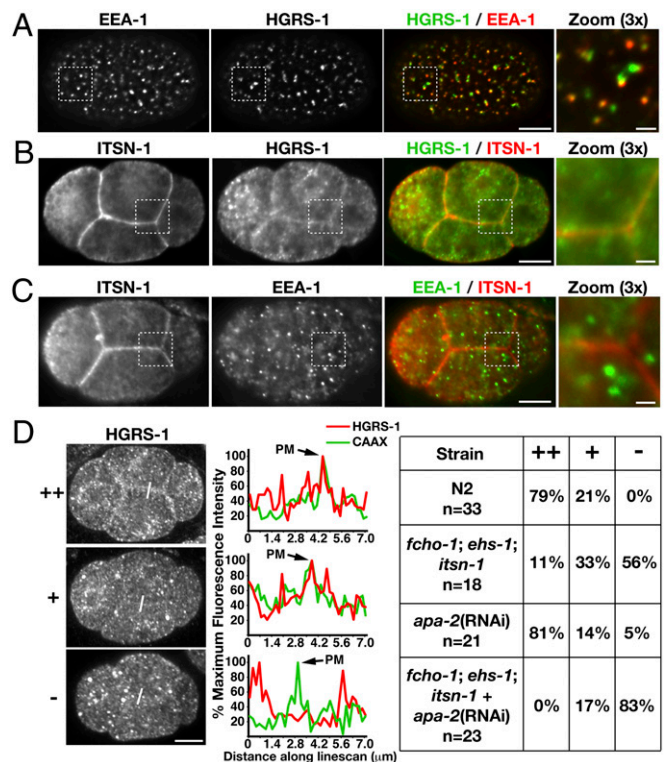


Fig. 3. ESCRT-0 localization to the plasma membrane depends on the presence of multiple endocytic adaptors. (A) One cell stage embryos were fixed and stained with directly labeled antibodies against HGRS-1 (Cy2) and EEA-1 (Cy3). Images (~4 μm from the coverslip) were acquired by using swept-field confocal optics. A 3 \times zoom of the boxed region is also shown (Right). (B and C) Four cell-stage embryos were fixed and stained with labeled antibodies against HGRS-1 (Cy2), EEA-1 (Cy2), or ITSN-1 (Cy3). Images (~9 μm from the coverslip) were acquired by using swept-field confocal optics. A 3 \times zoom of boxed regions is also provided (Right). (D) Four cell stage embryos expressing a GFP fusion to a CAAX motif (Fig. S5A) were fixed and stained by using antibodies directed against HGRS-1, and plasma membrane localization was quantified based on fluorescence intensity by using a linescan analysis (highlighted in each image). Peak fluorescence intensity of the GFP signal was used to define the localization of the plasma membrane. A table showing the relative intensity of HGRS-1 on the plasma membrane in different mutant backgrounds is shown on Right (++, high level of HGRS-1; +, low level of HGRS-1; -, an absence of HGRS-1). (Scale bars: A–D, 10 μm ; A–C Inset, 2 μm .)

of the evanescent field, strongly suggesting that ESCRT-0 continues to associate with clathrin-coated vesicles throughout the scission process (Fig. 4C and D). In contrast to the accumulation of ESCRT-0 at some clathrin-coated pits, we failed to observe the downstream ESCRT-I complex at these sites (Fig. 4E), consistent with the specific biochemical associations we identified among the ESCRT-0, FEI, and AP-2 complexes at the plasma membrane.

To further investigate whether ESCRT-0 accumulates at cargo-laden coated pits, we pulse labeled cells that were serum starved overnight with fluorescently labeled epidermal growth factor (EGF), followed by fixation. Cells were also pretreated with the dynamin inhibitor dynasore for 1 h before the brief (2 min) EGF stimulation, to ensure that membrane-associated EGF was restricted to the cell surface (Fig. S5C). Under these conditions, we found that YFP-Hrs accumulated at a subpopulation (~14%) of EGF-labeled sites (Fig. 4F; $n = 564$ sites analyzed). Collectively, our findings highlight a role for ESCRT-0 as an additional plasma membrane endocytic adaptor complex that functions during a subset of clathrin-mediated endocytosis events (Fig. 4G).

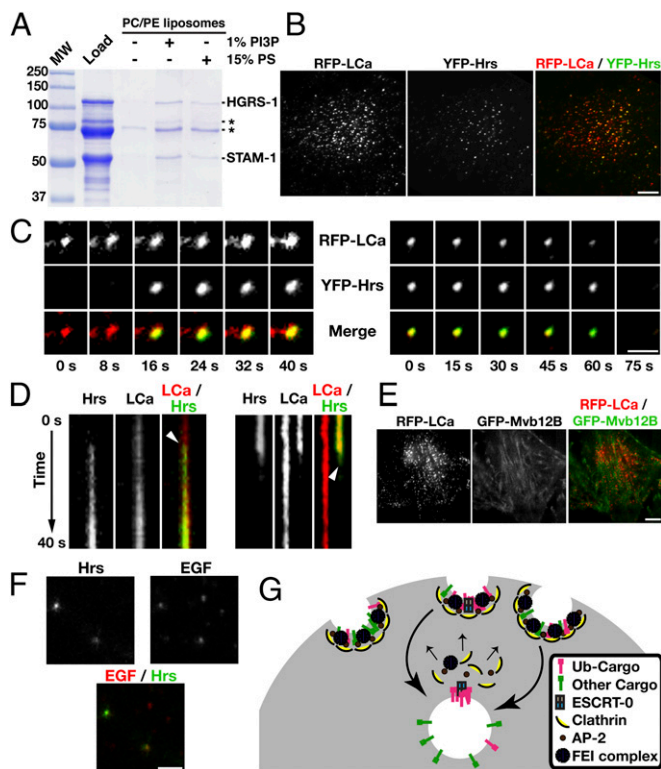


Fig. 4. ESCRT-0 associates with clathrin-coated pits at the plasma membrane. (A) Coflotation assays were conducted by using recombinant ESCRT-0 and liposomes containing either 70% phosphatidylcholine (PC) and 30% phosphatidylethanolamine (PE); 69% PC, 30% PE, and 1% PI3P; or 15% PS, 55% PC, and 30% PE. Asterisks highlight the presence of bacterial contaminants. (B) HeLa cells expressing RFP-clathrin light chain (LCa) and YFP-Hrs were imaged by using TIRF microscopy. (C) Individual sites of clathrin-mediated endocytosis were imaged over time by using TIRF microscopy. Merged panels showing both RFP-LCa and YFP-Hrs localization are shown (*Bottom*). (D) Kymographs showing the fate of RFP-LCa and YFP-Hrs at clathrin-coated pits over time. Arrows highlight the timing of Hrs appearance (*Left*) or disappearance (*Right*). (E) HeLa cells expressing RFP-clathrin light chain (LCa) and GFP-Mvb12B were imaged by using TIRF microscopy. (F) HeLa cells stably expressing YFP-Hrs were pretreated with dynasore (200 μ M) for 1 h and subsequently pulse-labeled with fluorescent EGF (10 ng/mL) for 2 min before fixation and imaging. (G) Model highlighting a role for ESCRT-0 in the capture of ubiquitin-modified cargoes at a subset of clathrin-coated pits. (Scale bars: B and E, 10 μ m; C and D, 2 μ m; F, 5 μ m.)

Discussion

Ubiquitin modification of transmembrane cargoes plays a key role in directing their entry into the endolysosomal system. At clathrin-coated pits, both Eps15 and epsin, which harbor motifs that associate weakly with ubiquitin, have been suggested to bind cargoes and potentially concentrate them before endocytosis (5). How these cargoes are then transferred efficiently to other ubiquitin-binding proteins at endosomes is difficult to envision. Our findings suggest that an alternative pathway exists to alleviate the need to resort cargoes following their arrival at endosomes. Specifically, we found that a component of the ESCRT machinery can associate directly with clathrin-coated pits, allowing it to engage ubiquitin-modified cargoes before their entry into the endosomal system. Furthermore, our data show that ESCRT-0 is present throughout the scission process, suggesting that cargoes remain bound to ESCRT-0 following internalization. In contrast, Eps15 and epsin arrive early to recruit and/or sequester ubiquitin-modified cargoes at clathrin-coated pits (10). Before internalization, ESCRT-mediated capture facilitates continued cargo clustering during vesicle transport and subsequent endosome fusion. Thus, preassembly of ESCRT-0 at nascent pits would enhance the

efficiency by which cargoes are sorted and, thereby, accelerate downstream trafficking steps, including ubiquitin-dependent degradation in lysosomes.

The role for ESCRT-0 at the cell surface may be similar to that of other factors that associate with clathrin-coated pits, but function at later steps of membrane transport. For example, the RME-6 exchange factor for Rab5 was shown previously to bind to the APA-2 subunit of the AP-2 complex. Although unlikely to function directly in vesicle formation, the presence of RME-6 at clathrin-coated pits likely enhances Rab5 activity, which is necessary for vesicle fusion with the endosome (35). In an analogous fashion, RME-4 also binds to APA-2 and activates Rab35, which functions later in cargo recycling (36). In *Drosophila* oocytes, components of the exocyst complex also associate with clathrin-coated pits (37). Although the association is dispensable during receptor internalization, the exocyst plays a key role in receptor recycling following endocytosis. Likewise, ESCRT-0 is unlikely to influence the process of clathrin-mediated endocytosis directly. Indeed, our data demonstrated that perturbations, which inhibit ESCRT-0 recruitment to the plasma membrane, fail to affect the rate of internalization of ubiquitin-modified cargoes. However, subsequent steps of cargo sorting were dramatically delayed. Collectively, these findings suggest that in addition to their specific roles in clathrin-mediated endocytosis, endocytic adaptor proteins also promote key priming events that prepare cargoes for downstream sorting.

Unlike the majority of clathrin adaptors studied to date, ESCRT-0 appears to associate with only a subpopulation of coated pits in human cells. Although its presence at additional sites of endocytosis may be below our detection limit, these data highlight the idea that all clathrin-coated pits are not uniform in composition. Instead, they may be strongly influenced by the presence of additional factors, such as cargo molecules (38). In particular, recent work suggests that ubiquitin can directly influence the maturation of a coated pit by acting as a signaling molecule in a dose-dependent fashion. Interestingly, the plasma membrane distribution of the mu opioid receptors, which undergo ubiquitin modification upon agonist stimulation, does not overlap uniformly with clathrin when activated, supporting the idea that multiple, distinct populations of clathrin-coated pits exist (39). These findings also raise the possibility that ubiquitin-mediated signaling during pit maturation is coupled to ESCRT-0 recruitment. Because membrane-associated ESCRT-0 is capable of binding at least eight ubiquitin molecules simultaneously (40), the localized enrichment of ubiquitin-modified cargoes at a subset of coated pits may help to specify the timing and/or site of its recruitment. Furthermore, the additional presence of endocytic adaptors, acidic phospholipids, and clathrin, all of which can associate with ESCRT-0, may further promote a level of coincidence detection that is necessary to enhance targeting to sites of clathrin-mediated endocytosis. This type of integration is likely important for the rapid and specific clearance of ubiquitin-modified cargoes, which is observed following receptor stimulation in human cells, as well as major changes to plasma membrane content following fertilization in *C. elegans*.

Materials and Methods

Antibodies, Immunofluorescence, and Live Imaging. *C. elegans* FCHO-1, EHS-1, and ITSN-1 antibodies were raised in rabbits, which were immunized with either a GST fusion to a fragment of FCHO-1 (amino acids 1–274), a GST fusion to a fragment of ITSN-1 (amino acids 1–283), or a polyhistidine-tagged form of full length EHS-1 produced in *Escherichia coli* and affinity purified. Antibodies directed against HGRS-1, STAM-1, EEA-1, APA-2, and RAB-5 have been described (40, 41). Confocal images were acquired on a swept-field confocal microscope (Nikon Ti-E), and TIRF imaging was conducted on a Nikon TE2000E equipped with a TIRF illuminator. Acquisition parameters and image analysis (including linescan analysis and the creation of kymographs) was performed by using Nikon Elements (confocal) or Metamorph (TIRF) software. Immunofluorescence of fixed embryos was performed as described (42) by using directly labeled rabbit antibodies at a concentration of 1 μ g/mL 30–40 Z sections at 0.2-mm steps were acquired (depending on sample thickness). To calculate the fluorescence intensity of specific proteins,

the total intensity in a box containing the signal (from a maximum intensity projection) was measured and the camera background was subtracted. For live imaging of *C. elegans*, animals were immobilized and mounted on an agarose pad. Alternatively, embryos were dissected from gravid animals and mounted for imaging. HeLa cells were grown on 35-mm glass bottom dishes maintained at 37 °C for time-lapse TIRF imaging. Treatments with dynasore were conducted as described (43).

Worm Strains, RNA Interference, and Cell Culture. All *C. elegans* strains were derived from the Bristol strain N2. The generation of animals expressing fluorescent fusions with CAV-1, MVB-12, and clathrin light chain were described (26, 42). Double-stranded RNA (dsRNA) was synthesized as described (42) from templates prepared by using specific primers to amplify N2 genomic DNA. For RNAi experiments, early L4 stage hermaphrodites were soaked in dsRNA for 24 h at 20 °C within a humidified chamber. Animals were allowed to recover for 48 h before analysis. HeLa cells were maintained in DMEM supplemented with 10% (vol/vol) FBS (HeLa), penicillin/streptomycin, and L-glutamine at 37 °C in the presence of 5% CO₂. Cells stably expressing a low level of YFP-Hrs were generated by retroviral infection, followed by fluorescence-activated cell sorting to isolate clonal populations, which were further sorted manually. Transfections were conducted by using FuGENE HD.

Mass Spectrometry, Biochemistry, and Liposome Flotation Assays. Adult hermaphrodites were grown synchronously in liquid culture, and embryonic

lysates were generated for immunoprecipitations as described (42). For mass spectrometry, proteins were precipitated by using TCA and were subsequently processed for MudPIT analysis (42). The spectra were searched with either the SEQUEST or ProLuCID (44) algorithm against the WormBase *C. elegans* database.

Recombinant protein expression was performed by using BL21 (DE3) *E. coli*, and purifications were conducted by using either glutathione agarose beads (for GST fusions) or nickel affinity resin (for polyhistidine-tagged proteins). Hydrodynamic studies and immunoblotting of extracts and immunoprecipitates were performed as described (42). To determine whether endogenous ESCRT-0 could interact with various fragments of recombinant EHS-1, ITSN-1, or FCHO-1, extracts were generated from embryos that were subsequently subjected to sonication in lysis buffer. Extracts were clarified by centrifugation (100,000 × g) before incubation with proteins bound to glutathione affinity resin. Coflotation assays were conducted as described (41).

ACKNOWLEDGMENTS. We thank Sun Lee for technical assistance. We also thank the Caenorhabditis Genetics Center and the National Bioresource Project (Japan) for sharing *C. elegans* mutant strains and members of the A.A. laboratory for critically reading this manuscript. This work was supported by National Institutes of Health Grants 1R01GM088151-01A1 (to A.A.) and P41RR011823 (to J.R.Y.).

- McMahon HT, Gallop JL (2005) Membrane curvature and mechanisms of dynamic cell membrane remodeling. *Nature* 438(7068):590–596.
- Field MC, Sali A, Rout MP (2011) Evolution: On a bender—BARs, ESCRTs, COPs, and finally getting your coat. *J Cell Biol* 193(6):963–972.
- McNiven MA, Thompson HM (2006) Vesicle formation at the plasma membrane and trans-Golgi network: The same but different. *Science* 313(5793):1591–1594.
- McMahon HT, Boucrot E (2011) Molecular mechanism and physiological functions of clathrin-mediated endocytosis. *Nat Rev Mol Cell Biol* 12(8):517–533.
- Reider A, Wendland B (2011) Endocytic adaptors—social networking at the plasma membrane. *J Cell Sci* 124(Pt 10):1613–1622.
- Traub LM (2009) Tickets to ride: Selecting cargo for clathrin-regulated internalization. *Nat Rev Mol Cell Biol* 10(9):583–596.
- Henne WM, et al. (2010) FCHO proteins are nucleators of clathrin-mediated endocytosis. *Science* 328(5983):1281–1284.
- Umasankar PK, et al. (2012) Distinct and separable activities of the endocytic clathrin-coat components Fcho1/2 and AP-2 in developmental patterning. *Nat Cell Biol* 14(5):488–501.
- Stimpson HE, Toret CP, Cheng AT, Pauly BS, Drubin DG (2009) Early-arriving Syp1p and Ede1p function in endocytic site placement and formation in budding yeast. *Mol Biol Cell* 20(22):4640–4651.
- Taylor MJ, Perrais D, Merrifield CJ (2011) A high precision survey of the molecular dynamics of mammalian clathrin-mediated endocytosis. *PLoS Biol* 9(3):e1000604.
- Reider A, et al. (2009) Syp1 is a conserved endocytic adaptor that contains domains involved in cargo selection and membrane tubulation. *EMBO J* 28(20):3103–3116.
- Mettlen M, et al. (2009) Endocytic accessory proteins are functionally distinguished by their differential effects on the maturation of clathrin-coated pits. *Mol Biol Cell* 20(14):3251–3260.
- Nunez D, et al. (2011) Hotspots organize clathrin-mediated endocytosis by efficient recruitment and retention of nucleating resources. *Traffic* 12(12):1868–1878.
- Cocucci E, Aguet F, Boulant S, Kirchhausen T (2012) The first five seconds in the life of a clathrin-coated pit. *Cell* 150(3):495–507.
- Kelly BT, Owen DJ (2011) Endocytic sorting of transmembrane protein cargo. *Curr Opin Cell Biol* 23(4):404–412.
- Bonifacino JS, Traub LM (2003) Signals for sorting of transmembrane proteins to endosomes and lysosomes. *Annu Rev Biochem* 72:395–447.
- Hicke L, Dunn R (2003) Regulation of membrane protein transport by ubiquitin and ubiquitin-binding proteins. *Annu Rev Cell Dev Biol* 19:141–172.
- Parachoniak CA, Park M (2009) Distinct recruitment of Eps15 via its coiled-coil domain is required for efficient down-regulation of the met receptor tyrosine kinase. *J Biol Chem* 284(13):8382–8394.
- Dores MR, Schnell JD, Maldonado-Baez L, Wendland B, Hicke L (2010) The function of yeast epsin and Ede1 ubiquitin-binding domains during receptor internalization. *Traffic* 11(1):151–160.
- Torrisi MR, et al. (1999) Eps15 is recruited to the plasma membrane upon epidermal growth factor receptor activation and localizes to components of the endocytic pathway during receptor internalization. *Mol Biol Cell* 10(2):417–434.
- Audhya A, McLeod IX, Yates JR, Oegema K (2007) MVB-12, a fourth subunit of metazoan ESCRT-I, functions in receptor downregulation. *PLoS ONE* 2(9):e956.
- Henne WM, Buchkovich NJ, Emr SD (2011) The ESCRT pathway. *Dev Cell* 21(1):77–91.
- Siegel LM, Monty KJ (1966) Determination of molecular weights and frictional ratios of proteins in impure systems by use of gel filtration and density gradient centrifugation. Application to crude preparations of sulfite and hydroxylamine reductases. *Biochim Biophys Acta* 112(2):346–362.
- Owen DJ, Collins BM, Evans PR (2004) Adaptors for clathrin coats: Structure and function. *Annu Rev Cell Dev Biol* 20:153–191.
- Koh TW, et al. (2007) Eps15 and Dap160 control synaptic vesicle membrane retrieval and synapse development. *J Cell Biol* 178(2):309–322.
- Sato K, et al. (2006) Dynamic regulation of caveolin-1 trafficking in the germ line and embryo of *Caenorhabditis elegans*. *Mol Biol Cell* 17(7):3085–3094.
- Hayer A, et al. (2010) Caveolin-1 is ubiquitinated and targeted to intraluminal vesicles in endolysosomes for degradation. *J Cell Biol* 191(3):615–629.
- Shi A, et al. (2009) Regulation of endosomal clathrin and retromer-mediated endosome to Golgi retrograde transport by the J-domain protein RME-8. *EMBO J* 28(21):3290–3302.
- Pan CL, et al. (2008) *C. elegans* AP-2 and retromer control Wnt signaling by regulating mig-14/Wntless. *Dev Cell* 14(1):132–139.
- Roxrud I, Raiborg C, Pedersen NM, Stang E, Stenmark H (2008) An endosomally localized isoform of Eps15 interacts with Hrs to mediate degradation of epidermal growth factor receptor. *J Cell Biol* 180(6):1205–1218.
- Raiborg C, et al. (2001) FYVE and coiled-coil domains determine the specific localization of Hrs to early endosomes. *J Cell Sci* 114(Pt 12):2255–2263.
- Gillooly DJ, et al. (2000) Localization of phosphatidylinositol 3-phosphate in yeast and mammalian cells. *EMBO J* 19(17):4577–4588.
- Kutateladze TG, et al. (2004) Multivalent mechanism of membrane insertion by the FYVE domain. *J Biol Chem* 279(4):3050–3057.
- Leventis PA, Grinstein S (2010) The distribution and function of phosphatidylserine in cellular membranes. *Annu Rev Biophys* 39:407–427.
- Sato M, et al. (2005) *Caenorhabditis elegans* RME-6 is a novel regulator of RAB-5 at the clathrin-coated pit. *Nat Cell Biol* 7(6):559–569.
- Sato M, et al. (2008) Regulation of endocytic recycling by *C. elegans* Rab35 and its regulator RME-4, a coated-pit protein. *EMBO J* 27(8):1183–1196.
- Sommer B, Oprins A, Rabouille C, Munro S (2005) The exocyst component Sec5 is present on endocytic vesicles in the oocyte of *Drosophila melanogaster*. *J Cell Biol* 169(6):953–963.
- Puthenveedu MA, von Zastrow M (2006) Cargo regulates clathrin-coated pit dynamics. *Cell* 127(1):113–124.
- Henry AG, et al. (2012) Regulation of endocytic clathrin dynamics by cargo ubiquitination. *Dev Cell* 23(3):519–532.
- Mayers JR, et al. (2011) ESCRT-0 assembles as a heterotetrameric complex on membranes and binds multiple ubiquitylated cargoes simultaneously. *J Biol Chem* 286(11):9636–9645.
- Kuwahara T, et al. (2008) A systematic RNAi screen reveals involvement of endocytic pathway in neuronal dysfunction in α -synuclein transgenic *C. elegans*. *Hum Mol Genet* 17(19):2997–3009.
- Witte K, et al. (2011) TFG-1 function in protein secretion and oncogenesis. *Nat Cell Biol* 13(5):550–558.
- Macia E, et al. (2006) Dynasore, a cell-permeable inhibitor of dynamin. *Dev Cell* 10(6):839–850.
- Xu T, et al. (2006) ProLuCID, a fast and sensitive tandem mass spectra-based protein identification program. *Mol Cell Proteomics* 5:5174.